

Effective Hamiltonian for $\text{Ga}_{1-x}\text{Mn}_x\text{As}$ in the Dilute Limit

Gregory A. Fiete,^{1,2,3} Gergely Zaránd,^{1,2,3} and Kedar Damle^{1,4}

¹*Department of Physics, Harvard University, Cambridge, Massachusetts 02138, USA*

²*Materials Science Division, Argonne National Laboratory, 9700 South Cass Avenue, Argonne, Illinois, 60429, USA*

³*Research Institute of Physics, Budapest University of Technology and Economics, Budapest H-1521, Hungary*

⁴*Department of Physics and Astronomy, Rice University, Houston, Texas 77005, USA*

(Received 6 December 2002; published 29 August 2003)

We derive an effective Hamiltonian for $\text{Ga}_{1-x}\text{Mn}_x\text{As}$ in the dilute limit, where $\text{Ga}_{1-x}\text{Mn}_x\text{As}$ can be described in terms of spin $F = 3/2$ polarons hopping between the Mn sites and coupled to the local Mn spins. We determine the parameters of our model from microscopic calculations. Our approach treats the large Coulomb interaction in a nonperturbative way, captures the effects of spin-orbit coupling and disorder, and is appropriate for other p -doped magnetic semiconductors.

DOI: 10.1103/PhysRevLett.91.097202

PACS numbers: 75.50.Dd, 75.30.Ds, 75.40.Gb

Since their discovery [1], dilute III–V magnetic semiconductors with high Curie temperatures have become the subject of very intense research [2]. Because the magnetic ions (usually Mn) responsible for the ferromagnetism are dissolved into the semiconductor itself, these materials could provide a unique opportunity to integrate ferromagnetic elements into larger, nonmagnetic, semiconducting devices.

In this Letter we focus on one of the most studied magnetic semiconductors, $\text{Ga}_{1-x}\text{Mn}_x\text{As}$, though most of our calculations carry over to other p -doped III–V magnetic semiconductors [3]. In $\text{Ga}_{1-x}\text{Mn}_x\text{As}$ substitutional Mn^{2+} play a fundamental role: They provide local spin $S = 5/2$ moments, and they dope holes into the lattice [4]. Since the Mn^{2+} ions are negatively charged compared to Ga^{3+} , in the very dilute limit they bind these holes, forming an acceptor level with a binding energy $E_b \approx 112$ meV [4]. As the Mn concentration increases, these acceptor states start to overlap and form an impurity band, which for even larger Mn concentrations merges with the valence band. Though the actual concentration at which the impurity band disappears is not known, according to optical conductivity measurements [5], this impurity band seems to persist at least up to nominal Mn concentrations of about $x \approx 0.05$. Angle resolved photoemission spectroscopy (ARPES) data [6,7] and the fact that even “metallic” samples feature a resistivity upturn at low temperature [8] also support the assertion that for smaller concentrations (and maybe even for relatively large nominal concentrations) one may be able to describe $\text{Ga}_{1-x}\text{Mn}_x\text{As}$ in terms of an impurity band [9].

In $\text{Ga}_{1-x}\text{Mn}_x\text{As}$ the Coulomb potential created by the Mn ions is by far the largest energy scale in the problem [10], but spin-orbit coupling in the hole band is also quite large compared to the exchange coupling between the holes and the Mn spins [4]. Fortunately, the large Coulomb potential of the Mn ion can be handled nonperturbatively. We construct a many-body Hamiltonian in this limit that captures spin-orbit effects, treats the large Coulomb interaction nonperturbatively, and incor-

porates the exchange coupling between the local moments and the holes.

The physics of the isolated Mn^{2+} + hole system is well understood [4]: In the absence of the Mn^{2+} core spin, the ground state of the bound hole at the acceptor level is fourfold degenerate and well described in terms of a $F = 3/2$ spin. For most purposes, we can restrict ourselves to this fourfold degenerate $F = 3/2$ acceptor level in the dilute limit. As also evidenced by infrared spectroscopy [4], the effect of the $S = 5/2$ Mn core spin is well described by a simple exchange Hamiltonian [2]:

$$H_{\text{exch}} = G \vec{S} \cdot \vec{F}, \quad (1)$$

with $G \approx 5$ meV [4].

The presence of other Mn sites has three important effects on the $F = 3/2$ acceptor state at any particular Mn site. (i) The Coulomb potential of the neighboring Mn^{2+} ions will induce a random *shift* E of the fourfold degenerate states. (ii) Because of the large spin-orbit coupling in GaAs, the neighboring atoms will also generate an anisotropy K and *split* the fourfold degeneracy of the $F = 3/2$ state into two doubly degenerate states. (iii) Finally, the presence of the neighboring ions will allow these $F = 3/2$ spin objects to *hop* between the Mn sites. However, this hopping t will *not conserve the spin* F because of the large spin-orbit coupling. Thus, in the dilute limit $\text{Ga}_{1-x}\text{Mn}_x\text{As}$ should be described by the following simple Hamiltonian:

$$H = \sum_{(i,j)} c_{i,\mu}^\dagger t_{ij}^{\mu\nu} c_{j,\nu} + \sum_i c_{i,\mu}^\dagger (K_i^{\mu\nu} + E_i \delta^{\mu\nu}) c_{i,\nu} + G \sum_{i,\mu,\nu} \vec{S}_i \cdot (c_{i,\mu}^\dagger \vec{F}_{\mu\nu} c_{i,\nu}), \quad (2)$$

where $c_{i,\nu}^\dagger$ creates a hole at the acceptor level [$F = 3/2, F_z = \nu$] at position i . As is clear from the arguments above, Eq. (2) is very general and appropriate for describing other p -doped III–V and II–IV semiconductors as well [3]. Hole-hole interactions can be incorporated in Eq. (2). In the metallic phase it is presumably a

good approximation to include only an on-site repulsion (discussed later) that eliminates double occupancy of the acceptor levels. In the localized phase, however, one may have to consider long-ranged hole-hole interactions.

To estimate the various parameters in Eq. (2), we studied the structure of the single impurity (Mn) and two-impurity (Mn_2) bound hole states using the so-called spherical approximation [11]. The top of the valence band in $\text{Ga}_{1-x}\text{Mn}_x\text{As}$ can be described in terms of spin $j = 3/2$ holes [12], whose spin couples strongly to their momenta. In the spherical approximation the motion of the holes in the Coulomb potential of an Mn ion is described by [11]

$$H_0 = \frac{\gamma}{2m}(p^2 - \mu \sum_{\alpha,\beta} J_{\alpha\beta} p_{\alpha\beta}) - \frac{e^2}{\epsilon r} + V_{cc}(r), \quad (3)$$

where $\gamma \approx 7.65$ is a mass renormalization parameter, m is the free electron mass, $\mu \approx 0.77$ is the strength of the spherical spin-orbit coupling in the $j = 3/2$ band [11], $\epsilon \approx 10$ is the dielectric constant of GaAs, and V_{cc} is the so-called central cell correction [13]. The spin-orbit term in Eq. (3) couples the momentum tensor of the holes $p_{\alpha\beta} = p_\alpha p_\beta - \delta_{\alpha\beta} p^2/3$ to their quadrupolar momentum, $J_{\alpha\beta} = (j_\alpha j_\beta + j_\beta j_\alpha)/2 - \delta_{\alpha\beta} j(j+1)/3$.

The bound states of H_0 (without the central cell correction) have been studied in the seminal paper [11]. Because of the spherical symmetry, the total momentum, $\vec{F} \equiv \vec{L} + \vec{j}$, is a conserved quantity, where \vec{L} is the orbital angular momentum. The ground state of H_0 is a fourfold degenerate $F = 3/2$ multiplet that contains a substantial d -wave contribution for GaAs due to the strong spin-orbit coupling. In Fig. 1 we illustrate the importance of this d -wave component by presenting the spatial dependence of the direction of hole polarization, $\vec{j}(\mathbf{r})$, for the state $|F = 3/2, F_z = 3/2\rangle$ which we calculated directly from the Baldereschi-Lipari wave functions with the central cell correction.

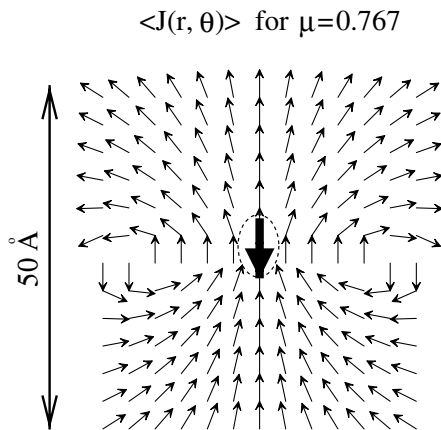


FIG. 1. Polarization direction of a bound hole in the state $|F = 3/2, F_z = 3/2\rangle$ in $\text{Ga}_{1-x}\text{Mn}_x\text{As}$ around a Mn ion (dark arrow pointing downwards represents the Mn $S = 5/2$ spin). Only the direction of the polarization is indicated. The magnitude falls off on a scale ~ 10 Å.

Having computed the single Mn hole states, we carried out a variational calculation to construct the molecular orbitals for a pair of Mn ions [3,14]. Since the exchange interaction with the Mn core spins is much smaller than the binding energy of the holes, we neglected the effect of G on their wave functions in these calculations. For the case where both the Mn-Mn bond and the quantization axis of F are parallel to the z axis, F_z is conserved and the spectrum of the lowest lying states of the molecule can be fully characterized by:

$$H_{\text{Mn-Mn}}^{\text{eff}} = \sum_{\nu} t_{\nu}(R)(c_{1,\nu}^{\dagger} c_{2,\nu} + \text{H.c.}) \quad (4)$$

$$+ \sum_{i=1,2} \left[K(R) \left(\nu^2 - \frac{5}{4} \right) + E(R) \right] c_{i,\nu}^{\dagger} c_{i,\nu}. \quad (5)$$

By time reversal symmetry, $t_{3/2} = t_{-3/2}$ and $t_{1/2} = t_{-1/2}$. All parameters depend only on the distance R between the two Mn sites (see Fig. 2). The most obvious effect of the spin-orbit coupling is that the hoppings $t_{3/2}$ and $t_{1/2}$ substantially differ from each other; holes that have their spin aligned with the Mn-Mn bond are more mobile. As indicated by the arrow, at the typical Mn-Mn distance for $x = 0.01$, K and $t_{1/2}$ can be entirely neglected compared to E and $t_{3/2}$. Therefore, in many cases it is enough to keep only the latter two terms in the effective Hamiltonian.

Having determined the effective Hamiltonian for a pair of Mn ions, we can use it to estimate the parameters in Eq. (2). Rotating the z axis along the bond direction \vec{n}_{ij} connecting sites i and j , we obtain $\mathbf{t}_{ij} = \mathcal{D}(\vec{n}_{ij}) \hat{\mathbf{t}}(R_{ij}) \mathcal{D}^{\dagger}(\vec{n}_{ij})$, $\mathbf{K}_i = \frac{1}{2} \sum_{j \neq i} K(R_{ij}) [(\vec{n}_{ij} \cdot \vec{F})^2 - \frac{5}{4}]$, and $E_i = \frac{1}{2} \sum_{j \neq i} E(R_{ij})$. Here $\mathcal{D}(\vec{n}_{ij})$ is a spin 3/2 rotation matrix, $\hat{\mathbf{t}}(R)$ denotes the diagonal matrix $\text{diag}(t_{3/2}(R), t_{1/2}(R), t_{1/2}(R), t_{3/2}(R))$, and R_{ij} denotes the distance between sites i and j .

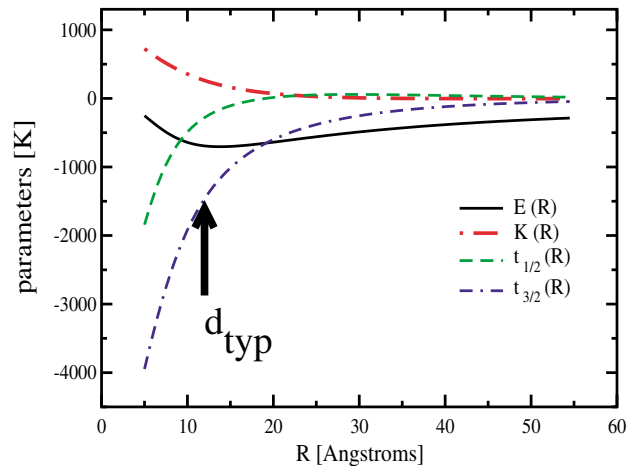


FIG. 2 (color online). Parameters of the two-impurity Hamiltonian Eq. (4) obtained from the variational study of two Mn ions. The arrow indicates the typical Mn-Mn distance, d_{typ} , for $x = 0.01$ Mn concentration.

Thus far we have neglected the interaction between holes. In the localized phase, however, this interaction may play an important role. In general, the Coulomb interaction between holes on different Mn sites has a very complicated form [3], though for large separations it simplifies considerably. Fortunately, the dominant interaction is the *on-site* hole-hole interaction. Within the spherical approximation this interaction can be expressed as

$$H_{\text{int}} = \frac{U_N}{2} \sum_i \hat{N}_i^2 + \frac{U_F}{2} \sum_i \hat{\mathbf{F}}_i^2, \quad (6)$$

where $\hat{N}_i = \sum_{\nu} c_{i,\nu}^{\dagger} c_{i,\nu}$, $\hat{\mathbf{F}}_i = \sum_{\mu,\nu} c_{i,\mu}^{\dagger} \vec{\mathbf{F}}_{\mu\nu} c_{i,\nu}$, and $:\cdots:$ denotes normal ordering. We estimated U_N and U_F in Eq. (6) by evaluating exchange integrals: $U_N = 2600$ K and $U_F = -51$ K.

Equations (2) and (6), together with the microscopic parameters of Fig. 2, constitute our central results. They provide a well controlled theoretical framework that captures the most important aspects of dilute magnetic semiconductors such as the localization phase transition, random anisotropy, disorder effects, and frustrated ferromagnetism. Postponing much of our detailed analysis to a longer publication [3], here we demonstrate the power of this model on only a few examples.

To obtain a better understanding of the model we first computed the ground state of four Mn atoms at a separation of 15 \AA due to the interaction mediated by a single hole on the cluster. We treated the Mn spins classically and used the simple mean field approximation of Ref. [9]. We considered only configurations where the Mn ions were positioned on a slightly distorted tetrahedron with three edges of length $a = 15 \text{ \AA}$ and three edges of length b (see Fig. 3). In all cases, in the ground state, the Mn spins are relatively collinear apart from a slight tilt of $5\text{--}10^\circ$. However, the spatial position of the Mn ions generates a strong anisotropy. Thus, the energy depends strongly on the directional orientation of the net spin

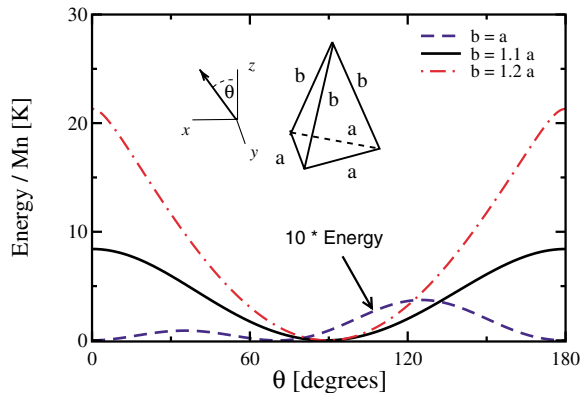


FIG. 3 (color online). Anisotropy induced by the distortion of a regular Mn tetrahedron in the presence of a single hole. The Mn-Mn distances are $a = 15 \text{ \AA}$ and $b = 15 \text{ \AA}$, $b = 16.5 \text{ \AA}$, and $b = 18 \text{ \AA}$, respectively. The distortion generated anisotropy can be almost 2 orders of magnitude larger than the undistorted anisotropy, which is of order 1 K/Mn.

relative to the underlying lattice. To demonstrate this we calculated the ground state energy as a function of the Mn spin direction (assuming full alignment). For a perfectly regular tetrahedron this anisotropy is rather small, less than 0.5 K/Mn. However, the anisotropy increases with the ratio b/a , and for $b/a = 1.2$ it can be as large as 20 K/Mn. In other words, random positions of the Mn ions induce a *random anisotropy* term that, depending on the disorder, is much larger than the bulk anisotropy, which is of the order of 1 K/Mn. Thus disorder and spin-orbit coupling together can induce a large random anisotropy energy comparable to T_C . These findings are in qualitative agreement with earlier results obtained in the metallic limit [15].

Finally, we discuss some of the results obtained for a $\text{Ga}_{1-x}\text{Mn}_x\text{As}$ of linear sizes $L = 10a_{\text{lat}}$ and $L = 13a_{\text{lat}}$ (with $a_{\text{lat}} = 5.65 \text{ \AA}$, the size of the conventional unit cell) and active Mn concentration $x_{\text{active}} = 0.01$, using the above-described mean field techniques at zero temperature. In the calculations presented below, we have not included the effects of Eq. (6). [This is partially justified *post facto* by Fig. 4 which shows that the states at the Fermi energy are delocalized.] We emphasize that x_{active} can be substantially less than the nominal Mn concentration, x , which also includes inactive Mn sites [16], and therefore these calculations may be relevant even for systems with larger nominal Mn concentration. The concentration of holes is also reduced compared to x due to strong compensation effects; we assumed that the number of holes is reduced by a factor of $f = 0.3$ relative to the number of Mn.

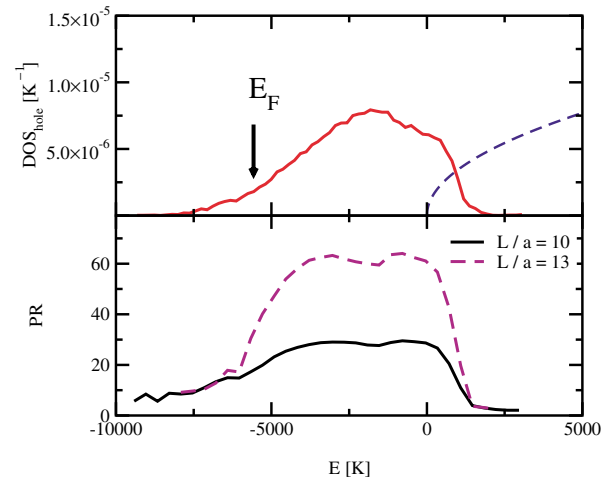


FIG. 4 (color online). Top: Computed average hole density of states per elementary cell for ten $L = 10a$ samples with $x = 0.01$ and $f = 0.3$. We also show the density of states of the valence band (dashed line). The Fermi energy is ≈ -6500 K. Bottom: The participation ratio for $L = 10a_{\text{lat}}$ and $L = 13a_{\text{lat}}$. States in the impurity band tails are localized while states in the middle are delocalized; states in the side tail above zero energy likely mix with the valence band states and are delocalized in reality.

To take into account correlations [10] induced between Mn ions during the experimental growth process, we introduced a screened Coulomb repulsion between the Mn ions and let them relax using $T = 0$ Monte Carlo simulations. For long times the Mn ions form a regular bcc lattice with some point defects. The data we present here are for intermediate times, where there is still appreciable disorder in the system.

Once we fixed the Mn positions in a given instance, we solved the mean field equations derived from (2) self-consistently [9]. We used periodic boundary conditions and implemented a short distance cutoff in the hopping parameters of Eq. (2) which corresponds to about eight neighbors for each Mn. The use of this cut off is justified by the observation that our molecular orbital calculations are only appropriate for “nearest neighbor” ion pairs and, in reality, holes cannot hop directly over the first “shell” of ions. We started from a configuration with fully aligned classical Mn spins, $\vec{\Omega}_i \equiv \vec{S}/S$, and then let the system relax to the nearest metastable state. Similar to the metallic case [15], we find a ferromagnetic state with a largely reduced magnetization, $|\langle \vec{\Omega}_i \rangle| \approx 0.4$ for $L = 10a_{\text{lat}}$. We find that this reduction is largely due to spin-orbit coupling, and that the cosine of the angle θ between the spins and the ground state magnetization has a broad distribution similar to the metallic case [15].

The density of states is shown in Fig. 4. The half-width of the impurity band is about 0.2 eV at this density, which slightly overlaps with the valence band density of states. However, comparison with the valence hole density of states suggests that at this concentration a well-formed impurity band may still be present, and it might persist to higher concentrations. Indeed, this scenario seems to be supported by many experiments [5,6].

The impurity band has a tail of localized states that reaches inside the band gap. These states can be identified for various system sizes. [See Fig. 4 wherein the participation ratio (PR), $\text{PR} = [\sum_i (\sum_\alpha |\psi_{i\alpha}|^2)^2]^{-1}$, grows with system size for delocalized states while the PR remains $O(1)$ in the thermodynamic limit for localized states].

This tail gradually disappears when we introduce correlations between the Mn ions which tend to form regular structures [3]. In agreement with ARPES data [6], we find that the chemical potential lies deep (~ 0.5 eV) inside the gap. From the PR data, it appears that the chemical potential is in the vicinity of the mobility edge, a regime where our model is probably more reliable. This raises the interesting possibility that the localization phase transition in $\text{Ga}_{1-x}\text{Mn}_x\text{As}$ could happen inside the impurity band and that the ferromagnetic phase for smaller Mn concentrations is governed by localized hole states [10,17].

Though our calculations are based on microscopic model calculations, they are only approximate, and more

realistic *ab initio* calculations would be needed to give a quantitative answer concerning the role of the impurity band. Also, though the spherical approximation we used is able to reproduce rather well the spectrum of a single acceptor, it probably overestimates the effect of spin-orbit coupling, and also the width of the impurity band.

In summary, based on microscopic calculations we constructed a many-body Hamiltonian that is appropriate for describing $\text{Ga}_{1-x}\text{Mn}_x\text{As}$ in the dilute limit. We find that the hopping of the carriers is strongly correlated with their spin. This spin-dependent hopping is crucial for capturing spin-orbit coupling induced random anisotropy terms, the lifetime of the magnon excitations, and for capturing the universality class of the localization phase transition. Our calculations suggest the presence of an impurity band for $x_{\text{active}} = 0.01$ Mn concentration.

We are grateful to B. Jankó, M. Berciu, R. Bhatt, A. H. MacDonald, P. Schiffer, and especially J. K. Furdyna, X. Liu, and E. Sasaki for stimulating discussions. This research has been supported by the U.S. DOE, Office of Science, NSF Grants No. DMR-9985978 and No. DMR97-14725, and Hungarian Grants No. OTKA F030041, No. T038162, and No. N31769. G.Z. is a Bolyai fellow.

-
- [1] H. Ohno, *Science* **281**, 951 (1998).
 - [2] J. König *et al.*, in *Electronic Structure and Magnetism of Complex Materials*, edited by D.J. Singh and D.A. Papaconstantopoulos (Springer-Verlag, Berlin, 2002); R. N. Bhatt *et al.*, *J. Supercond.* **15**, 71 (2002); T. Dietl, *cond-mat/0201282*.
 - [3] G. Fiete, G. Zaránd, and K. Damle (unpublished).
 - [4] M. Linnarsson *et al.*, *Phys. Rev. B* **55**, 6938 (1997).
 - [5] E. J. Singley *et al.*, *Phys. Rev. Lett.* **89**, 097203 (2002).
 - [6] H. Åsklund *et al.*, *Phys. Rev. B* **66**, 115319 (2002).
 - [7] J. Okabayashi *et al.*, *Phys. Rev. B* **64**, 125304 (2001).
 - [8] A. Van Esch *et al.*, *Phys. Rev. B* **56**, 13103 (1997).
 - [9] M. P. Kennett, M. Berciu, and R. N. Bhatt, *Phys. Rev. B* **66**, 045207 (2002).
 - [10] C. Timm, F. Schäfer, and F. von Oppen, *Phys. Rev. Lett.* **89**, 137201 (2002).
 - [11] A. Baldereschi and N.O. Lipari, *Phys. Rev. B* **8**, 2697 (1973).
 - [12] W. Kohn and J. M. Luttinger, *Phys. Rev.* **98**, 915 (1955).
 - [13] A. K. Bhattacharjee and C. Benoit á la Guillaume, *Solid State Commun.* **113**, 17 (2000).
 - [14] A. C. Durst, R. N. Bhatt, and P. A. Wolff, *Phys. Rev. B* **65**, 235205 (2002).
 - [15] G. Zaránd and B. Jankó, *Phys. Rev. Lett.* **89**, 047201 (2002).
 - [16] K. M. Yu *et al.*, *Appl. Phys. Lett.* **81**, 844 (2002); K. M. Yu *et al.*, *Phys. Rev. B* **65**, 201303 (2002).
 - [17] S.-R. Yang and A. H. MacDonald, *Phys. Rev. B* **67**, 155202 (2003).